



# E-Field Strength Measurement using Rydberg Atom Based sensor for Microwave Metrology

H. S. Rawat <sup>(1,2)</sup>, D. Kara <sup>(3)</sup>, T. Firdoshi <sup>(3)</sup>, S. Garain <sup>(3)</sup>, S. K. Dubey <sup>(1,2)</sup>, A. K. Mohapatra <sup>(3)</sup>, and V. N. Ojha <sup>(1,2)</sup>

(1) Academy of Scientific and Innovative Research (AcSIR), Ghaziabad-201002, India

(2) CSIR-National Physical Laboratory, Dr. K. S. Krishnan Marg, New Delhi-110012, India

(3) School of Physical Sciences, National Institute of Science Education and Research, Bhubaneswar, Homi Bhabha National Institute, Jatni-752050, India

## Abstract

In this work, the theoretical and measurement results have been reported of microwave E-field sensing using an atomic spectroscopy instead of conventional methods (using antennae) under practice till date. This method is based on interaction of microwave with the Rb atoms excited to the Rydberg states by using two laser beams. This significantly new technique may get accepted internationally as a new primary standard for accurate and precise measurements of various Radio-Frequency parameters such as E-field, power, radiation pressure etc as it provides traceability to physical constants and SI units. The atomic model is also studied theoretically and Optical Bloch equations of the same are reported. It has been shown that microwave E-field strength is measured by studying the frequency difference between the peaks in laser transmission curve. The ability of atoms to sense E-field is shown by varying the power and distance of the antenna from atomic cell. In addition, results are shown for weak RF field detection by detuning the RF field by MHz order.

## 1. Introduction

Recently, International Bureau of Weights and Measures (BIPM) has decided to redefine all the basic SI units in terms of the physical constants which describe the natural world. This decision initiated research in all departments of science to make all the derived units traceable to either SI units or to physical constants. The metrological institutes across the world have proved that the atom-based metrological techniques provide more accurate, precise and reproducible results as compared to the conventional techniques. The atom-based standards have been accepted worldwide for measurement of time, frequency, gravity, magnetometry, and length [1]–[3]. To date, the RF E-field sensing and calibration techniques does not have traceability to physical constants and have complex traceability path. The dependency on the materials under use, limitation of bandwidth of antennae under use, the surrounding parameters at the time of measurement, and the incorrect evaluation of uncertainties are some of the limitations of current techniques which makes measurable quantity vulnerable to the errors.

The technique discussed in this work has many promising benefits over the conventional techniques such as the dependency of dipole antennae (having limited bandwidth of operation) as a reference probe can be replaced by atomic cell which can sense RF E-fields from few MHz to 500 GHz and beyond [4]–[6]. The atoms provide self-calibrating measurements due the invariance in atomic resonances, enhanced sensitivity can be achieved of the order of  $1 \mu\text{V m}^{-1} \text{ Hz}^{-1/2}$  [5]. The field will not be perturbed by the metallic probes as the field is sensed by atomic transitions in this technique.

This technique is based on the interaction of the highly excited alkali atoms with RF energy and utilizes the concepts of quantum interference phenomena like Electromagnetically Induced Transparency (EIT) [7], [8] and Autler-Townes Splitting (ATS) [9]. The Rydberg atoms have a huge response to the external E-field which helps in converting the E-field amplitude measurement to the optical-frequency response. The discussed work may find its application in accurate measurement of E-field amplitude which plays a crucial role in the determination of many other parameters such as Specific Absorption Rate (SAR) in biomedical application, EMI/EMC testing of RF and electronic devices, non-invasive RF based detection and diagnostic medical devices, etc.

## 2. Atomic Model and Experimental Setup

To measure microwave amplitude via Rydberg atoms a Rb vapor cell is placed as shown in the schematic of the experimental setup in Fig. 1 (a). The counter-propagating linearly co-polarized laser beams interact with the atoms in the presence of microwave (MW) illuminated from the transverse direction to the line of direction of propagation of laser fields by using Rohde & Schwarz SMR40 with the help of co-axial to waveguide adapter (hp P281C). The weak probe laser of 780.24 nm with  $2.7 \mu\text{W}$  is produced by TOPTICA DL-Pro which tunes the ground state  $5S_{1/2} \rightarrow 5P_{3/2}$ . Another laser of 480.044 nm with 136 mW is produced by TOPTICA-TA-SHG Pro is scanned to couple the atomic states  $5P_{3/2} \rightarrow 5D_{5/2}$  and will be referred to as control laser throughout this article. The probe laser is locked by SAS technique with the help of TOPTICA Digilock, and

control laser is amplitude modulated using chopper to increase signal-to-noise ratio and the result in modulation of probe transmission is observed with lock-in amplifier. The transmission of the probe laser is continuously monitored with photodetector APD 120A. Figure 1 (b) shows the atomic ladder model depicting the transitions.

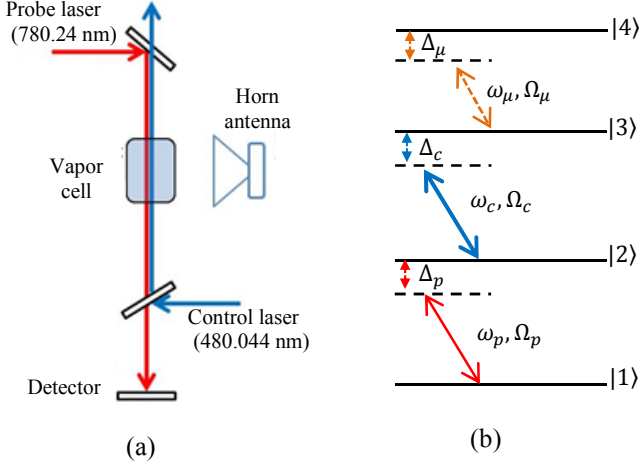


**Figure 1.** (a) Representational setup for the atomic transitions based E-field metrology; (b) Energy level structure of the atom.

When only probe laser passes through atomic ensemble the atoms absorb most of the light and a very weak light gets detected but when a strong coupling laser with higher Rabi frequency interacts with the same atoms an enhancement in the transmission of probe light is observed. This enhancement in transmission of probe signal is known as Electromagnetically Induced Transparency (EIT) which occurs due to interference between the atomic states.

The interaction of another electromagnetic field *i.e.* MW in EIT regime gives rise to Autler-Townes split of the EIT peak [4], [10]. This further split of the transparency window is exploited for the SI traceable atomic standard for MW electric-field amplitude measurement. In a recent work, we have reported that MW allows an additional level for interference and results in Double Electromagnetically Induced Transparency (DEIT) in which the transparency window splits in two with a rise of a third peak at center [10].

The evolution of the system with time can be determined by writing the equations of motion in the interaction picture and under rotating-wave approximation and can be written as

$$\begin{aligned} \dot{\rho}_{21} &= -\left(\frac{\Gamma_{21}}{2} + i\Delta_p\right)\rho_{21} + \frac{i}{2}\Omega_p + \frac{i}{2}\Omega_c\rho_{31}, \\ \dot{\rho}_{31} &= -\left(\frac{\Gamma_{31}}{2} + i(\Delta_p + \Delta_c)\right)\rho_{31} + \frac{i}{2}\Omega_\mu\rho_{41} \\ &\quad + \frac{i}{2}\Omega_c\rho_{21} - \frac{i}{2}\Omega_p\rho_{32}. \end{aligned} \quad (1)$$

$$\begin{aligned} \dot{\rho}_{41} &= -\left(\frac{\Gamma_{41}}{2} + i(\Delta_p + \Delta_c + \Delta_\mu)\right)\rho_{41} \\ &\quad + \frac{i}{2}\Omega_\mu\rho_{31} - \frac{i}{2}\Omega_p\rho_{42}. \end{aligned}$$

where the parameters  $\Delta_p = \omega_p - \omega_{12}$ ,  $\Delta_c = \omega_c - \omega_{23}$ ,  $\Delta_\mu = \omega_\mu - \omega_{34}$ ,  $\Delta_{\mu 2} = \omega_{\mu 2} - \omega_{34}$  are the detunings of the applied probe, control, and two MW fields respectively with  $\omega_{ij}$  the on-resonance angular frequency for the state  $i$  to  $j$  transition, and spontaneous decay rates ( $\gamma_{ij}$ ) from the upper state  $i$  to lower state  $j$ .

Solving this set of equations by applying the weak probe conditions, the imaginary part of  $\rho_{12}$  can be calculated, which can be further used to evaluate susceptibility as

$$Im(\chi)|_{dopp.} = \frac{1}{v_p\sqrt{2\pi}} \int e^{-v^2/v_p^2} Im(\chi) dv \quad (2)$$

where  $v_p$  is the most probable speed,  $v$  is the velocity of atoms, and  $Im(\chi)$  is the imaginary part of susceptibility which can be evaluated by

$$Im(\chi) = \frac{2|d_{ij}|^2 dn}{\hbar \epsilon_0 \Omega_p} \rho_{12}^{Im} \quad (3)$$

where  $dn$  is the atomic density in per  $\text{cm}^3$ ,  $d_{ij}$  is the dipole moment of the transition, and other parameters have their usual meaning. The transmission of the probe light through the atomic vapor can then be expressed as

$$T = \frac{I}{I_0} = e^{-\alpha l} \quad (4)$$

Where  $\alpha$  is the absorption coefficient given by  $\alpha = Im(\chi)\omega/c$ ,  $l$  is the length of vapor cell,  $\omega$  is the frequency of laser beam. By observing the above expression, the incident MW E-field strength can be determined by measuring the separation between the two peaks in the probe absorption spectrum which can be evaluated by

$$E_\mu = 2\pi\Delta f \frac{\hbar}{d_\mu} \quad (5)$$

where  $\hbar$  is the Planck's constant,  $\Delta f$  is the splitting in the transmission peak, and  $d_{rf}$  is the atomic dipole moment of the MW transition and can be evaluated by utilizing the quantum defects of  $^{85}\text{Rb}$  [4], [11]. The calculation of atomic dipole moment can be evaluated by the expression  $d_\mu = eA_{34}R_{34}$  which further depends on the calculation of angular ( $A_{34}$ ) and radial part ( $R_{34}$ ).  $A_{34}$  is calculated to be 0.4899 for the transition from  $nD_{5/2} \rightarrow (n+1)P_{3/2}$  states which is the case considered in this article for measurements, the radial part can also be evaluated from the analysis given in [4].

### 3. Results and Discussions

The theoretical probe transmission evaluated for various values of MW Rabi frequencies are shown in Figure 2 (a-d). Figure 2(a) shows the EIT peak when MW is switched off and only probe and control laser fields interact with the atoms with Rabi frequencies  $\Omega_p = 1$  MHz and  $\Omega_{\mu c} = 4$

MHz respectively. Figure 2(b), (c), and (d) represents the split in the EIT peak when MW is illuminated on the atoms in EIT regime for the cases  $\Omega_\mu = 1\text{MHz}$ ,  $\Omega_\mu = 2\text{MHz}$ , and  $\Omega_\mu = 5\text{MHz}$  respectively. This split is utilized to evaluate E-field by measuring the frequency difference ( $\Delta f$ ) between the two peaks and by substituting  $\Delta f$  in expression (5) the amplitude of the incident MW can be estimated.

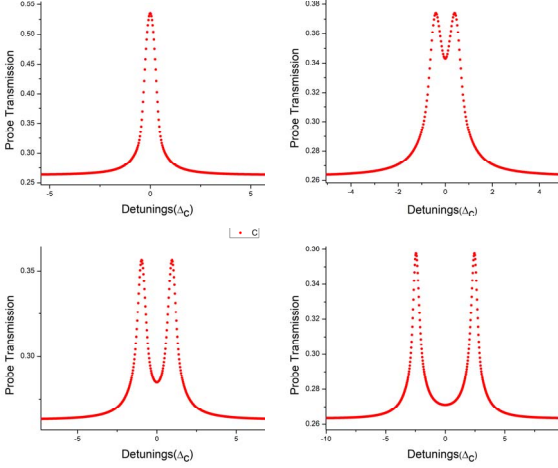


**Figure 2.** Probe transmission versus control detuning ( $\Delta_c$ ). (a) MW OFF; EIT observed for weak probe beam; (b)  $\Omega_\mu = 1\text{MHz}$ ; (c)  $\Omega_\mu = 2\text{MHz}$ ; (d)  $\Omega_\mu = 5\text{MHz}$ .

The experimental probe transmission signal with respect to the probe detuning through the vapor cell in the presence of different values for RF power is shown in Figure 3. Figure 3(a) represents the case when only the two laser fields are acting on the Rb atoms and MW field is switched off. The two transmission peaks correspond to the two closely spaced Rydberg states  $52D_{3/2}$  and  $52D_{5/2}$ . The energy difference between the two states is calculated and measured to be 83 MHz [12].

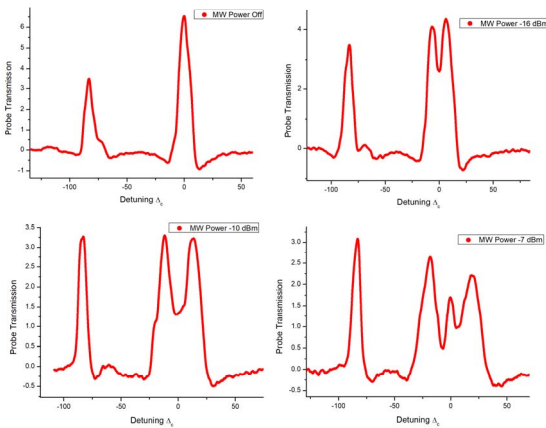


**Figure 3.** Probe transmission versus control detuning ( $\Delta_c$ ) in MHz for (a) MW OFF; EIT peaks for the states  $52D_{3/2}$  and  $52D_{5/2}$ ; (b) MW is ON and is set to resonance with 15.0971 GHz and power -16 dBm; (c) MW power is -10 dBm; (d) MW power is -7 dBm.

The calculated frequency detunings and E-field strengths for various power levels are given in Table 1. Figure 3(b)

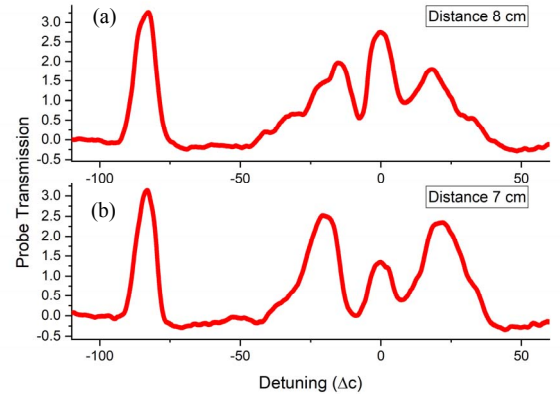
represents the case when MW field is switched ON and interacts with the Rydberg states in the EIT regime. The MW field of 15.0971 GHz and power level of -16 dBm is illuminated by co-axial to waveguide adapter from the distance of 9 cm. The split in EIT curve corresponds to the destructive interference between the atomic pathways. The  $\Delta f$  measured from the experimental data is 12.659 MHz which corresponds to the Electric-field strength of 564.08 mV/m.

Figure 3(c) is for the case when incident RF power is -10 dBm for fixed MW frequency. The  $\Delta f$  measured for the blue curve from the experimental data is 24.969 MHz which corresponds to the Electric-field strength of 1.112 V/m. Similarly, the  $\Delta f$  for Figure 3(d) is calculated to be 37.256 MHz which corresponds to the Electric-field strength of 1.660 V/m for the MW power of -7 dBm. One may easily notice the rise of the third peak at the center of EIT window when MW power is increased and is believed to be the transition from EIT to Double EIT.

Figure 4 showcases the two different behaviors in the transmission of probe light when the distance of antenna is 8 cm (Figure 4(a)) and 7 cm (Figure 4(b)) from the vapor cell. The power of the MW is -7 dBm for both the cases keeping frequency and other parameters same as were in Figure 3. The calculated E-field strengths for the two cases are 1.4817 V/m and 1.8116 V/m respectively. In addition, the pattern of the transmission curves agrees well with the cases presented in our earlier work [10]. It has also been shown that the presence of the third peak can be utilized in the polarization vector determination of the MW field in the presence of external magnetic field [13, 14].

**Table 1.** Calculated frequency detuning and E-field strength for various power levels of incident MW field

| Power variation | $\Delta f$ (MHz) | F-field amplitude (V/m) |
|-----------------|------------------|-------------------------|
| -16 dBm         | 12.659           | 0.564                   |
| -10 dBm         | 24.969           | 1.112                   |
| -7 dBm          | 37.256           | 1.660                   |



**Figure 4.** Probe transmission versus control detuning ( $\Delta_c$ ) in MHz for different values of distance of antenna from vapor cell. (a)  $d = 8\text{ cm}$ ; (b)  $d = 7\text{ cm}$ .

Next, the response of the probe transmission curve is shown when the frequency of MW is detuned to the lower side of the transition. The power level and position of the antenna is fixed to -17 dBm and 9 cm respectively for both the cases. It has been observed that detuning of the field induces asymmetry in the EIT curve which agrees well with the findings reported in [15]. The difference between the heights of the two peaks increases with the increase in detuning. This behavior of curves can be utilized to sense very weak fields which may not give distinct split in the EIT curve but when detuned, the asymmetry help in easily calculating the  $\Delta f_0$ . The split in peak with MW detuning can be calculated by the expression [15]

$$\Delta f_\delta = \sqrt{\delta_\mu^2 + \Delta f_0^2} \quad (6)$$

where  $\Delta f_\delta$  is the separation between the peaks when MW field is detuned from the actual transition,  $\delta_\mu$  is detuned frequency of MW field, and  $\Delta f_0$  is the peak separation when MW is at its actual transition frequency. The  $\Delta f_0$  can be evaluated for the case of weak field from expression (6) by substituting the values of  $\Delta f_\delta$  and  $\delta_\mu$  from the measurement data. Figure 5(a) and (b) represents the case when MW is detuned by -4 MHz and -10 MHz respectively. By substituting the value of  $\Delta f_\delta$  from experimental data in expression (6) the value of  $\Delta f_0$  obtained is 10.099 MHz which corresponds to E-field strength of 494.58 mV/m by using expression (5).

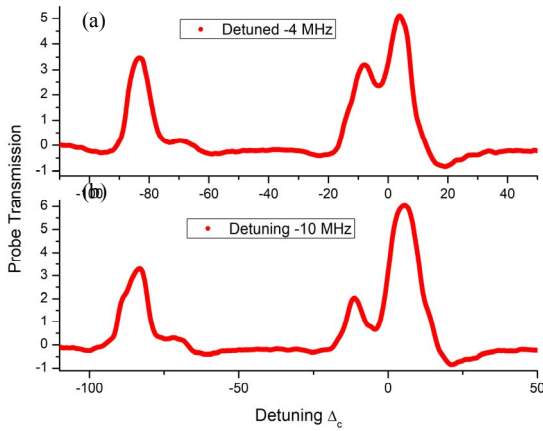


**Figure 5.** Probe transmission versus control detuning ( $\Delta_c$ ) in MHz for left detuning of the MW field. (a)  $f_\mu = 15.0931$  GHz, detuned by 4 MHz from resonance; (b)  $f_\mu = 15.0871$  GHz, detuned by 10 MHz from resonance.

The sources of uncertainties in the experiment are currently under study. Some of the possible sources of uncertainties in this method are: 1) variation in the linewidth of the probe transmission curves; 2) walls of vapor cell can absorb or reflect the microwaves; 3) the evaluation of MW dipole moment. 4) the evaluation of energy difference between the Rydberg states. Moreover, some more work has to be done to test the sensitivity of the atomic sensor. The direction dependence of the incident MW field is yet to be done.

## 4. Acknowledgement

H. S. Rawat, S. K. Dubey and V. N. Ojha are thankful to Science and Engineering Research Board (SERB), Department of Science and Technology (DST), Government of India, Confederation of Indian Industry (CII) and Rohde & Schwarz India Pvt. for Prime Minister Fellowship for Doctoral Research. D. Kara, T. Firdoshi, S. Garain and A. K. Mohapatra are thankful to Department of Atomic Energy (DAE) for financial support.

## 5. References

- [1] H. Fan, S. Kumar, J. Sedlacek, H. Kübler, S. Karimkashi, and J. P. Shaffer, "Atom based RF electric field sensing," *J. Phys. B At. Mol. Opt. Phys.*, vol. 48, no. 20, 2015.
- [2] M. Koschorreck, M. Napolitano, B. Dubost, and M. W. Mitchell, "Sub-Projection-Noise Sensitivity in Broadband Atomic Magnetometry," *Phys. Rev. Lett.*, vol. 104, no. 9, p. 93602, Mar. 2010.
- [3] W. Wasilewski, K. Jensen, H. Krauter, J. J. Renema, M. V. Balabas, and E. S. Polzik, "Quantum Noise Limited and Entanglement-Assisted Magnetometry," *Phys. Rev. Lett.*, vol. 104, no. 13, p. 133601, Mar. 2010.
- [4] C. L. Holloway *et al.*, "Broadband Rydberg Atom-Based Electric-Field Probe: From Self-Calibrated Measurements to Sub-Wavelength Imaging," vol. 62, no. 12, pp. 6169–6182, 2014.
- [5] C. L. Holloway *et al.*, "Atom-Based RF Electric Field Metrology: From Self-Calibrated Measurements to Subwavelength and Near-Field Imaging," *IEEE Trans. Electromagn. Compat.*, vol. 59, no. 2, pp. 717–728, 2017.
- [6] M. T. Simons, J. A. Gordon, and C. L. Holloway, "Simultaneous use of Cs and Rb Rydberg atoms for dipole moment assessment and RF electric field measurements via electromagnetically induced transparency," *J. Appl. Phys.*, vol. 120, no. 12, 2016.
- [7] S. E. Harris, "Electromagnetically Induced Transparency," *Opt. Photonics News*, vol. 2, no. 12, p. 29, 2009.
- [8] M. Fleischhauer, A. Imamoglu, and J. P. Marangos, "Electromagnetically induced transparency: Optics in coherent media," *Rev. Mod. Phys.*, vol. 77, no. 2, pp. 633–673, 2005.
- [9] C. H. Autler, S. H. Townes, "Stark effect in rapidly varying fields," *Phys. Rev.*, vol. 100, no. 2, pp. 703–722, 1955.
- [10] H. S. Rawat, S. K. Dubey, and V. N. Ojha, "Distinction between double electromagnetically induced transparency and double Autler-Townes splitting in RF-driven four-level ladder  $87\text{Rb}$  atomic vapor," *J. Phys. B At. Mol. Opt. Phys.*, vol. 51, no. 15, 2018.
- [11] I. I. Sobelman, *Atomic Spectra and Radiative Transit*, Second. New York: Springer US, 1992.
- [12] A. K. Mohapatra, T. R. Jackson, and C. S. Adams, "Coherent Optical Detection of Highly Excited Rydberg States Using Electromagnetically Induced Transparency," *Phys. Rev. Lett.*, vol. 98, no. 11, p. 113003, Mar. 2007.
- [13] J. A. Sedlacek, A. Schwettmann, H. Kübler, and J. P. Shaffer, "Atom-based vector microwave electrometry using rubidium rydberg atoms in a vapor cell," *Phys. Rev. Lett.*, vol. 111, no. 6, pp. 1–5, 2013.
- [14] H. S. Rawat, S. K. Dubey, and V. N. Ojha, "Polarization Dependence of Interferences inside Rb Atomic Vapor Governing Microwave Vector E-field Metrology," *J. Opt. Soc. Am. B*, 36, 3547-3544, 2019.
- [15] M. T. Simons, J. A. Gordon, C. L. Holloway, D. A. Anderson, S. A. Miller, and G. Raithel, "Using frequency detuning to improve the sensitivity of electric field measurements via electromagnetically induced transparency and Autler-Townes splitting in Rydberg atoms," *Appl. Phys. Lett.*, vol. 108, no. 17, 2016.